Nanoscale phase separations in correlated materials by micro-XANES

RICMASS

50. Zakopane School of Physics
breaking frontiers: submicron structures in physics and biology

**A. Marcelli INFN - LNF**
USTC - NSRL & RICMASS
marcelli@lnf.infn.it

May 19, 2015

Layout

INFN
Istituto Nazionale
di Fisica Nucleare

- **Introduction**
- **phase separation scenario and mesophysics**
- **why we need μ-XANES mapping?**
- **percolative mechanisms and superconductivity**
- **conclusions**

*Zakopane, May 19, 2015*

MULTISCALE PHASE SEPARATION

Control and manipulation of multiscale phase separation from

Atomic scale →
Molecular scale →
Nanoscale →
Mesoscale →
**Microscale →**

Energy

Time
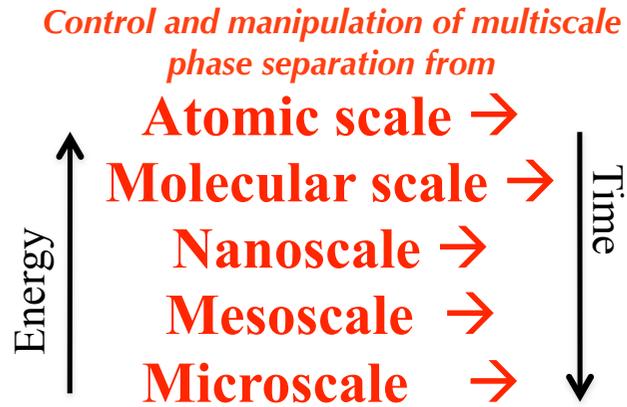
may determine new fundamental material functionality in many challenging open problems in

Energy
Biology & Biomedicine
Nanotechnology
**Environmental science**
Fundamental science
....
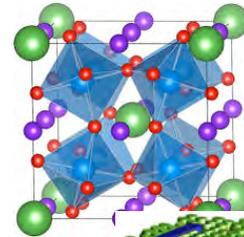
perovskites
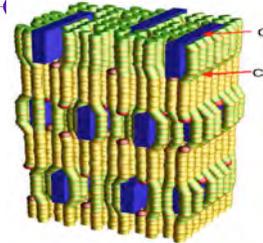
bone
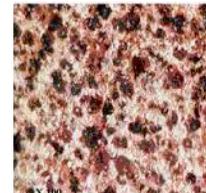
chocolate
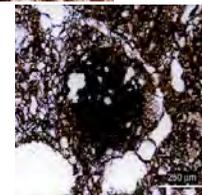
soils
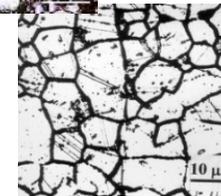
steel

HETEROSTRUCTURES AT ATOMIC LIMIT
Atomic layers intercalated by space layers
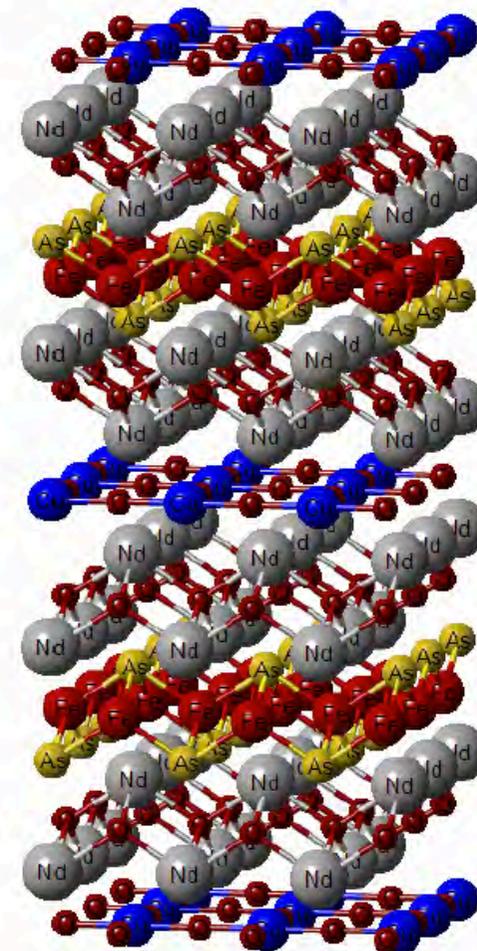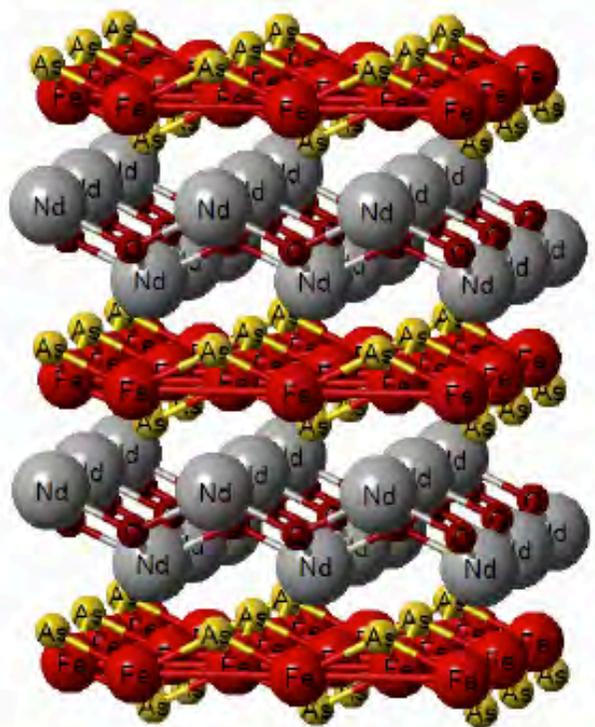
A. Ricci, et al. , Superconductor Science and Tech. 23, 052003 (2010)

Experiments probing the local structure have already shown in 90's that the structure of the metallic CuO_2 plane in high Tc cuprate superconductors is not homogeneous at a mesoscopic scale length

This work supported the interpretation of the anomalous electronic and transport properties of cuprate superconductors with the "two component" model. In fact the large tilting and the elongation of the in-plane Cu-O distances in the distorted Cu sites indicated that the electronic structure in the D stripes is different from that in the U stripes. The heterostructure of the CuO_2 plane at optimum doping supports the amplification of the superconducting critical temperature in cuprates. In this system, the itinerant charges are confined in a superlattice of quantum wires of width L [~16 Å] and period [~25 Å].

However, is not easy to reconcile horizontal or vertical spin stripes with the diagonal lattice stripes in the oxygen ion sublattice due to the existence of different contributions such as the polaron self-organization, the lattice parameter misfit strain and the self-organization of dopants in the spacer layers. The understanding of these complex stripe-topology require ultimate techniques like micro/nano XRD and micro/nano XANES, that may support the reconstruction of the "network structure" at the atomic scale.

Zakopane, May 19, 2015
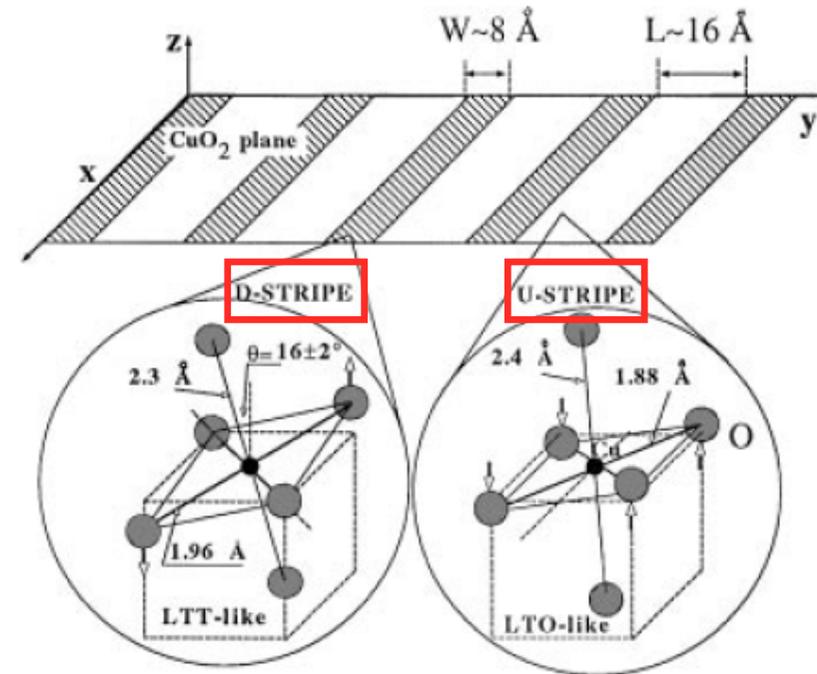
X-RAY ABSORPTION SPECTROSCOPY

Local and partial empty density of states

Cross section

$$\sigma(\omega) = 4\pi^2 \alpha \hbar \omega \sum_{\mathrm{if}} \{ |\langle \mathrm{f}|\hat{\varepsilon} \cdot r|\mathrm{i}\rangle|^2$$

$$+ (1/4)|\langle \mathrm{f}|\hat{\varepsilon} \cdot r\, k \cdot r|\mathrm{i}\rangle|^2 \} \delta(E_{\mathrm{f}} - E_{\mathrm{i}} - \hbar\omega).$$

Only dipole and electric quadrupole terms are considered

$$\sigma(\omega) = \sigma_\alpha(\omega)\,[1 + \chi(\omega)] = \sigma_\alpha(\omega) + \sigma_\alpha(\omega)\,\chi(\omega)$$

How it works?

Zakopane, May 19, 2015
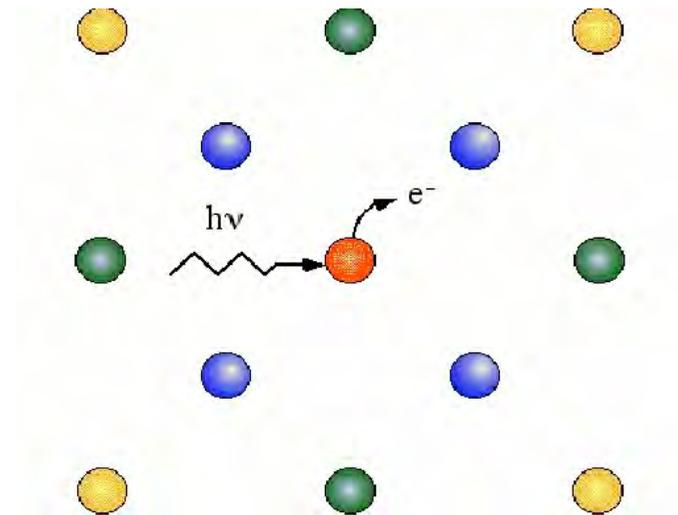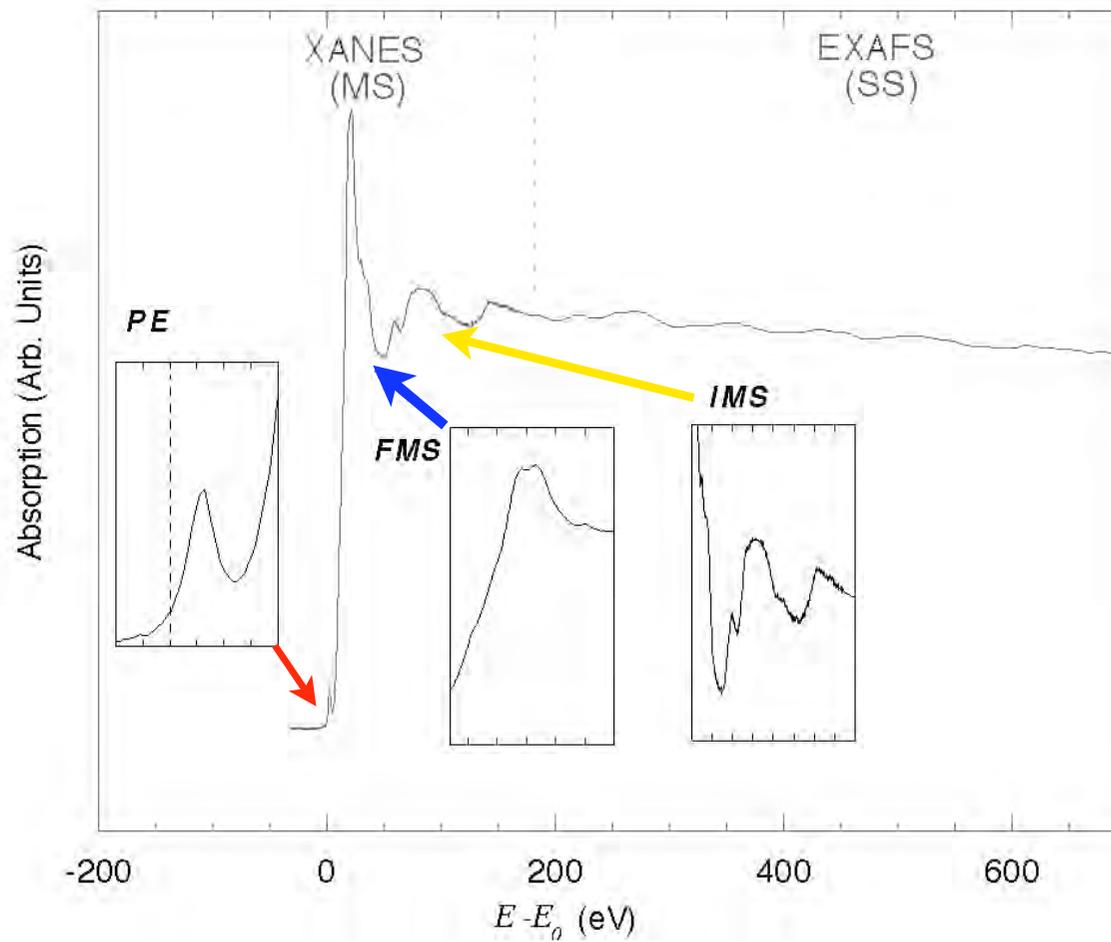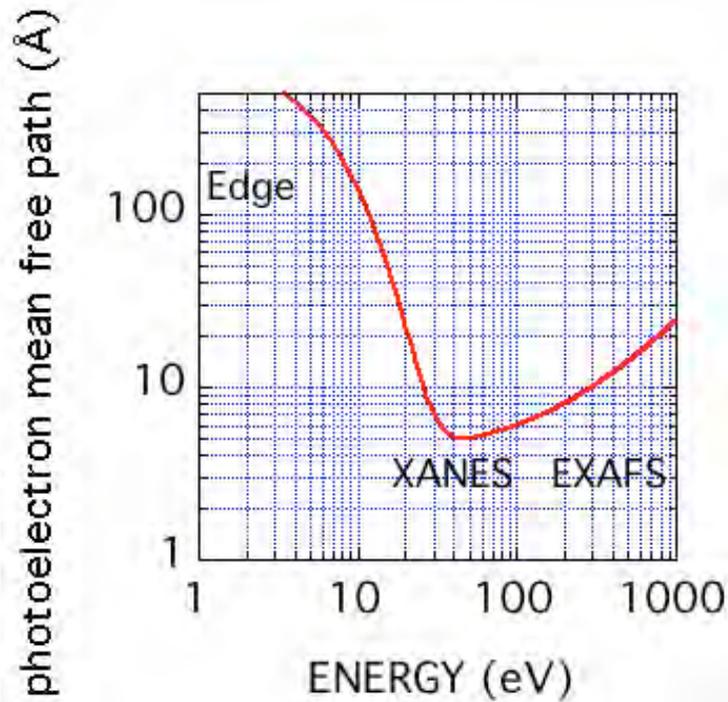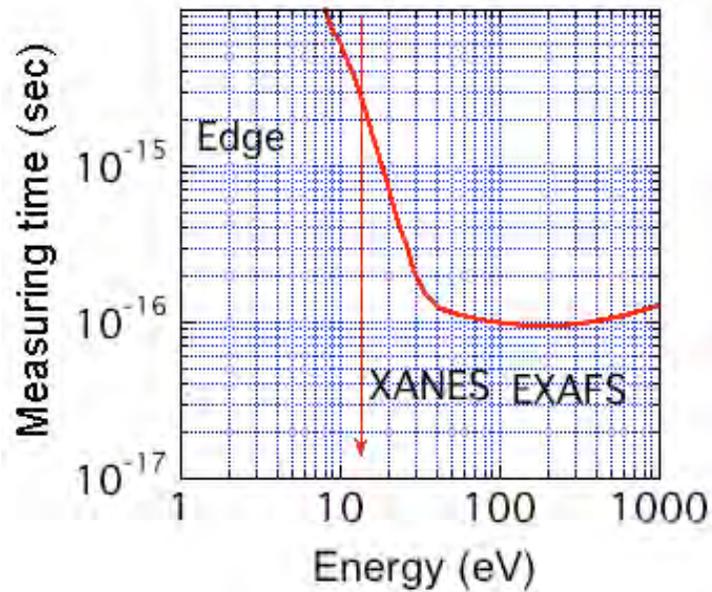
- **The life time of an excited electron above the chemical potential with kinetic energy E becomes very short.**

- **EXAFS and XANES probe the local lattice in the femtosecond time scale**

F. Meirer, J. Cabana, Yijin Liu, A. Mehta,
J. C. Andrews and P. Pianetta
Three-dimensional imaging of chemical phase
transformations at the nanoscale with full-
field transmission X-ray microscopy
J. Synchrotron Rad. (2011) 18, 773–781

Chemical RGB phase map for Li-ion
battery electrode sample (red = NiO,
green = Ni, blue = mixed states);

Panels (b) and (c) show the comparison of
XANES from two pixels with linear
combination fits, residual and quality of fit
R-factor.

(b) XANES -> 80% NiO, 20% Ni
(c) XANES -> 19% NiO and 81% Ni.

(d) normalized XANES of NiO and Ni:
electrode (pure NiO) and reduced electrode
(pure Ni).

SSRL - X-ray microscope @ BL6-2

Zakopane, May 19, 2015
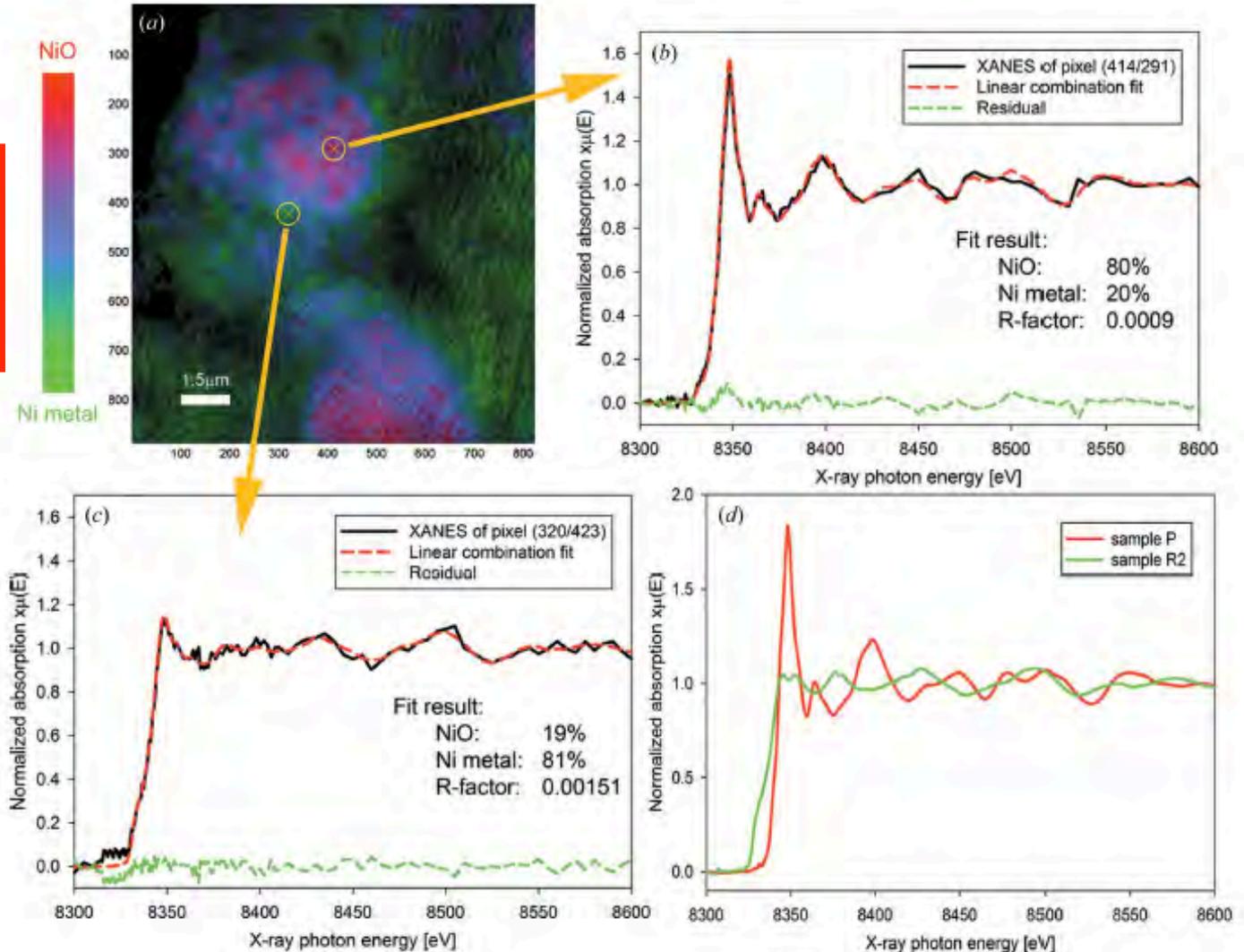
XANES spectroscopy

Being a fast (10^{-15} s) and local probe (few Å) of a selected atomic species, which also does not require a long range order, XANES spectroscopy represents an almost unique spectroscopic technique. Using extremely small spots, without space averaging, it is suited to investigate the local structure and the electronic properties of different polymorphs, systems with vacancies/impurities/defects, materials where complex magnetic, electronic and structural phase separations occur.

Zakopane, May 19, 2015
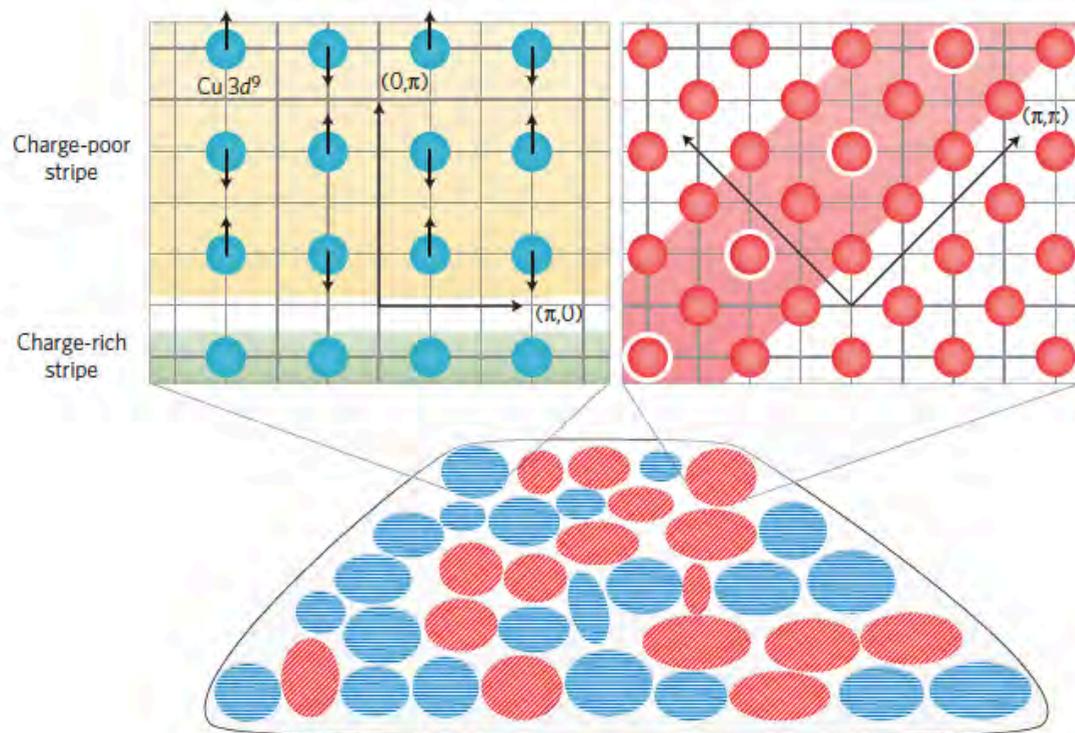
The XANES technique is really powerful when applied to investigate the nature of a **multi-scale correlated system**: **a system with a multi-scale structure and dynamics**, unavoidably entangled among them well beyond the manifold nature of a disordered system.

Complex lattice architectures can be associated to **transition metals and RE oxides and** to many **superconductors** such as cuprates or pnictides, all systems where a rich variety of **nanoscale structural, electronic and magnetic phases** may coexist.

The interplay of nano- and micrometer-scale factors is typically at the origin of the macroscopic behavior of these systems so that the capability to **probe morphology and phase distribution in complex systems at multiple length scales** is mandatory.

The superstripes scenario in the CuO₂ plane of cuprate heterostructures can be described by this picture where the complex existing phase separation forms different networks characterized by different types of puddles. Above, blue puddles indicates magnetic regions and red ones those superconducting.
Top left: Magnetic puddles comprise horizontal (or vertical) spin stripes in the Cu sublattice (blue dots), with spin indicated by black arrows. Top right: Superconducting puddles are made of diagonal lattice stripes in the oxygen sublattice (red dots) with rows of oxygen interstitials (white circles) in the spacer layers, and charge-rich stripes (red shading) intercalated by charge-poor stripes.

Zakopane, May 19, 2015

disordered phase of oxygen interstitials in the spacer layers after rapid quenching
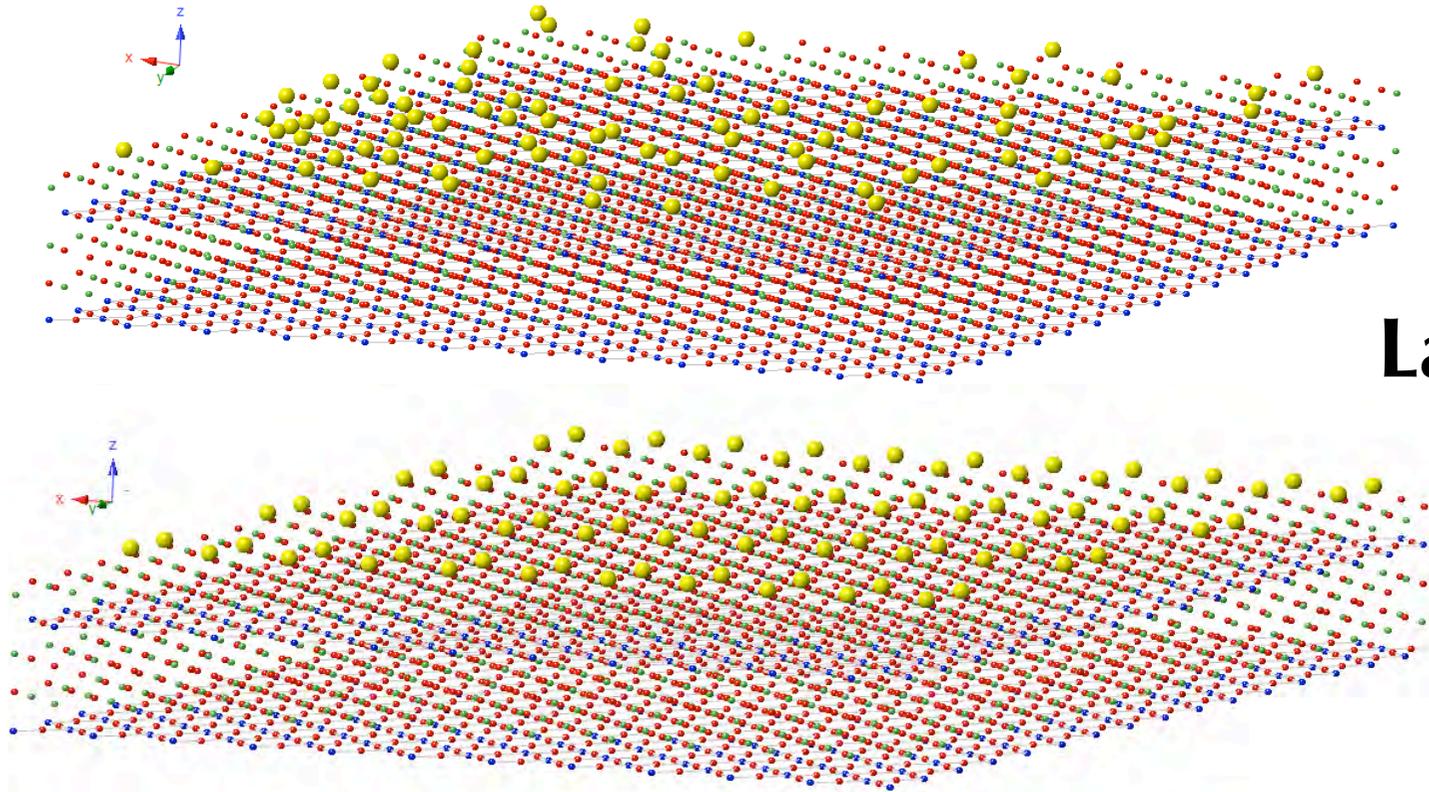
La_2CuO_{4+y}

3D ordered domains of oxygen interstitials in the spacer layers after annealing

Zakopane, May 19, 2015

Scale-free structural organization of oxygen interstitials in La$_2$CuO$_{4+y}$

Michela Fratini[1]†, Nicola Poccia[1], Alessandro Ricci[1], Gaetano Campi[1,2], Manfred Burghammer[3], Gabriel Aeppli[4] & Antonio Bianconi[1]

Zakopane, May 19, 2015
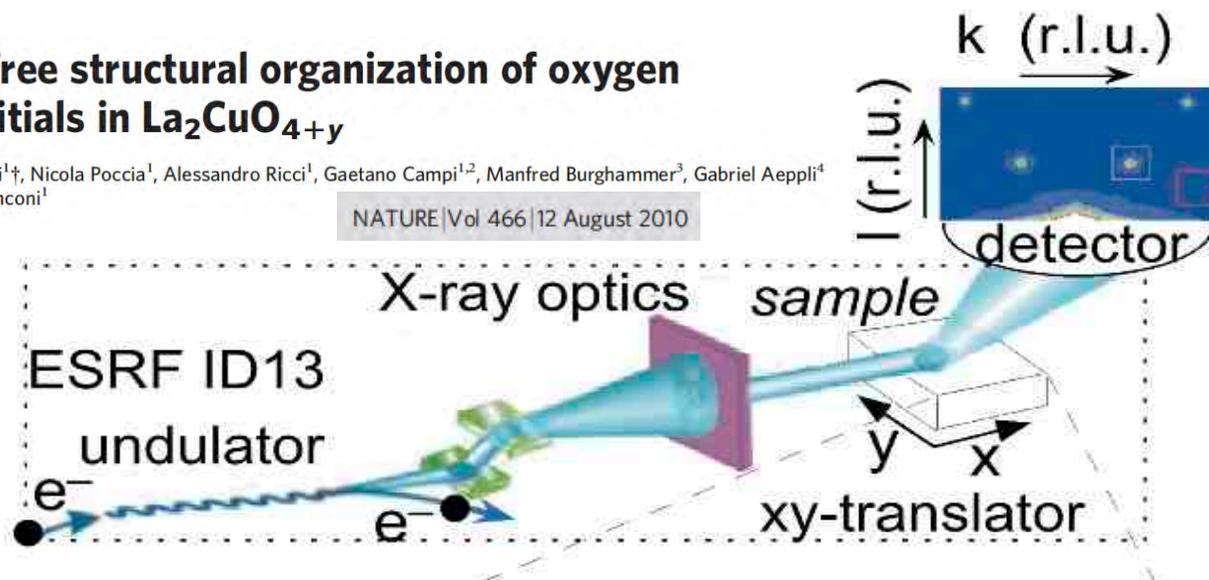
The complex "microstructures" of correlated materials such as TM oxides and high-T_c cuprate superconductors and the presence of oxygen interstitials (Oi) or vacancies tune the bulk properties. Actually, Oi present in the spacer layers separating the CuO_2 planes undergo ordering phenomena in $Sr_2O_{1+y}CuO_2$, $YBa_2Cu_3O_{6+y}$ and La_2CuO_{4+y} increasing T_c with no changes in hole concentrations.

In LaCuO has been shown the presence of a scale-free fractal distribution and a power-law behavior associated to Oi ordered domains. On the right - the position dependence of the Q2 superstructure intensity for two samples obtained with different annealing–quenching protocols: the phase with Tc~40 K (a) and the phase with Tc~16+32 K (b). The probability distribution P(x) of the Q2 XRD intensity scales at sufficiently high intensity as a power-law distribution with a cut-off X_0 independent by the sample critical temperature while the cut-off increases from 7-9 for the low Tc sample to 28-33 for the high Tc sample.
This work points out also that the misfit strain parameter of the superlattice copper oxides is similar to many other heterogeneous TM oxides. In addition, the superconductivity is associated with the critical percolation of oxygen order (optimal inhomogeneities).

Scale-free structural organization of oxygen interstitials in La_2CuO_{4+y}

Michela Fratini[1]†, Nicola Poccia[1], Alessandro Ricci[1], Gaetano Campi[1,2], Manfred Burghammer[3], Gabriel Aeppli[4] & Antonio Bianconi[1]

Random network

Zakopane, May 19, 2015
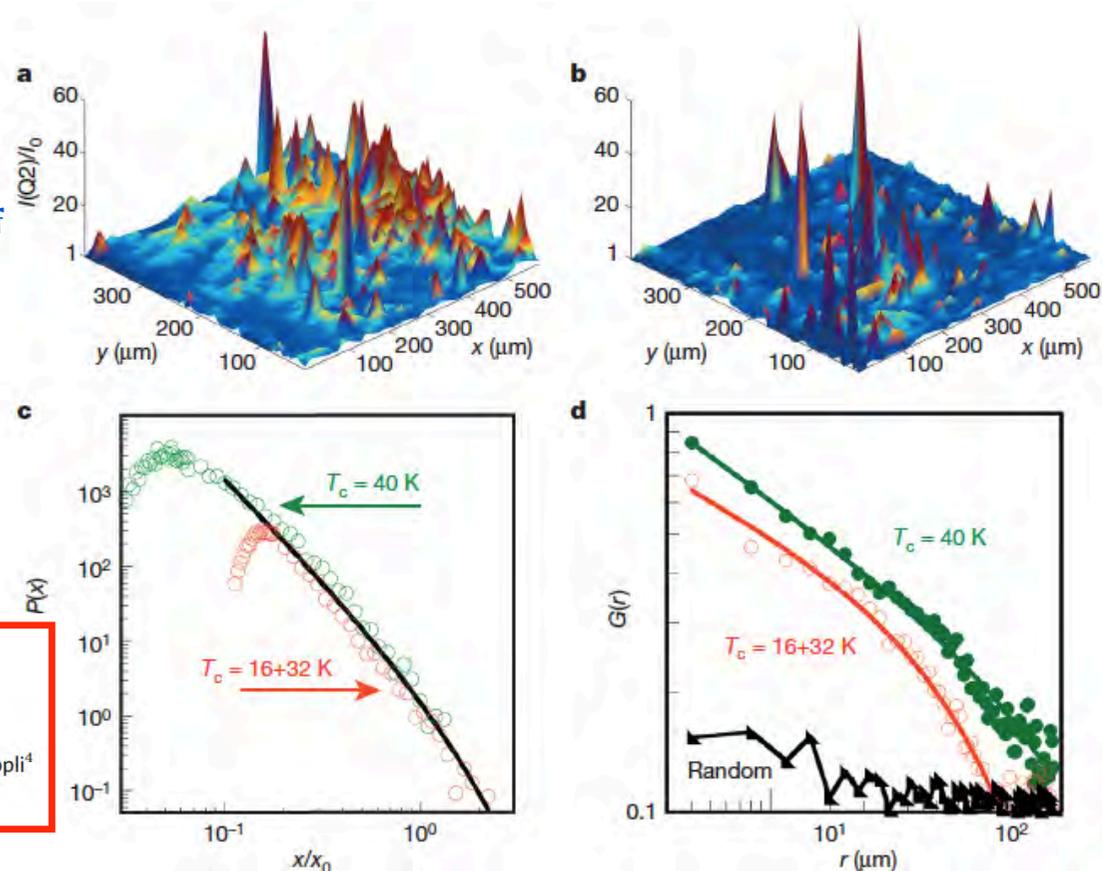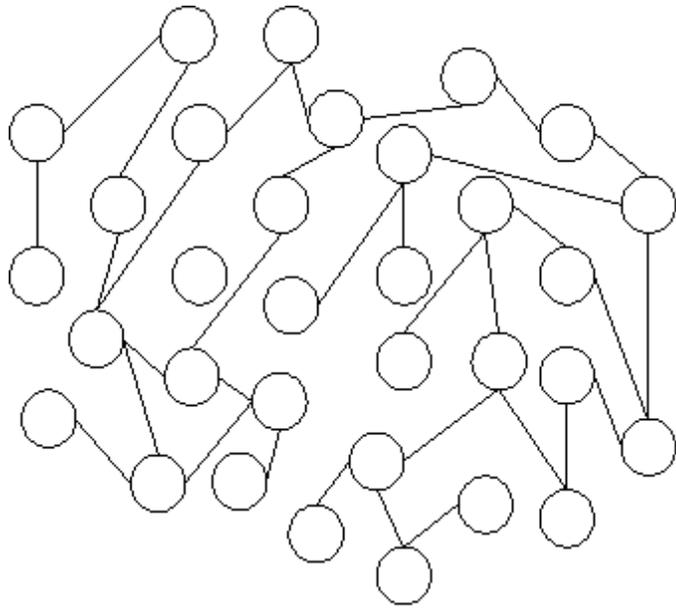
Even in optimal superconducting samples the oxygen defect order can be highly inhomogeneous. Actually, the glue regions contain incommensurate modulated local lattice distortions, whose spatial extent is most pronounced for the best superconducting samples. For an underdoped single crystal with mobile oxygen interstitials in the spacer La_2O_{2+y}, the incommensurate modulated local lattice distortions form droplets anticorrelated with the ordered Oi. In the simplest among high temperature superconductors, two networks of ordered defects coexist. They can be tuned to achieve optimal superconductivity.
Actually, for a given stoichiometry, the highest transition temperature is obtained when both the ordered oxygen (Oi) and the lattice defects (LLD) form fractal patterns.
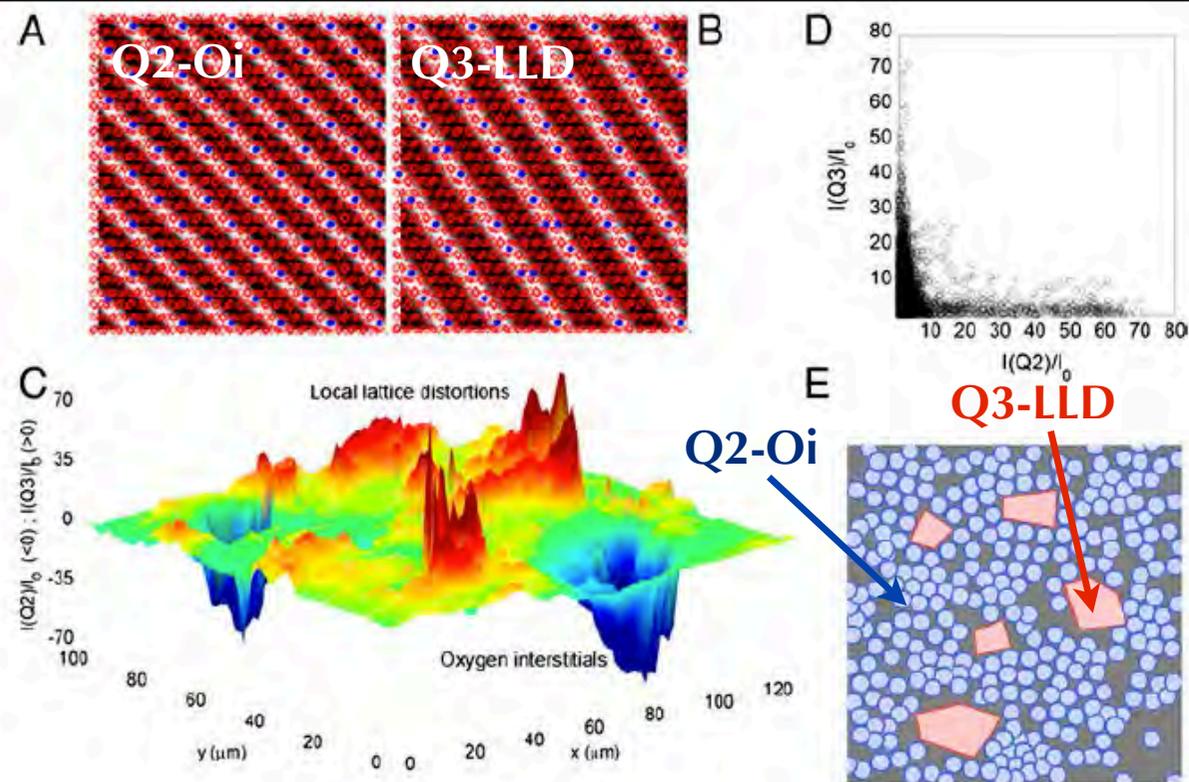
# Optimum inhomogeneity of local lattice distortions in La_2CuO_{4+y}

Nicola Poccia[a,b], Alessandro Ricci[a,c], Gaetano Campi[d], Michela Fratini[a,e], Alessandro Puri[f], Daniele Di Gioacchino[f], Augusto Marcelli[f], Michael Reynolds[b], Manfred Burghammer[b], Naurang Lal Saini[a], Gabriel Aeppli[g], and Antonio Bianconi[a,h,i,1]

Zakopane, May 19, 2015

Oi	Oxygen interstitials sitting at the sitting at the (¼,¼, ¼) interstitial site position in the K_2NiF_4 lattice structure
Q2-Oi	Self organization of oxygen interstitials with superlattice wave-vector $q2 = 0.25 \ \mathbf{b}* + 0.5c*$
LLD	Local Lattice distortions
Q3-LLD	Self organization of local lattice distortions with superlattice wave-vector $q3 = 0.21 \ \mathbf{b}* + 0.29c*$
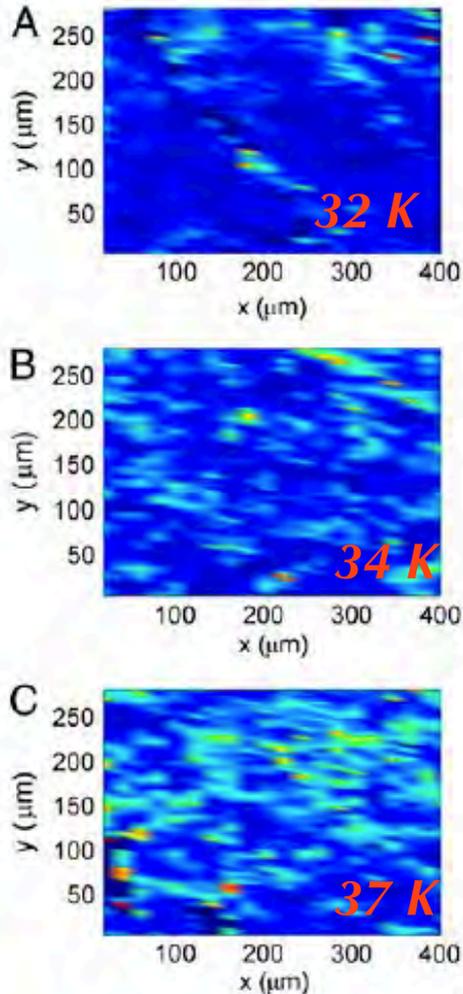
Q3-LLD vs. Tc
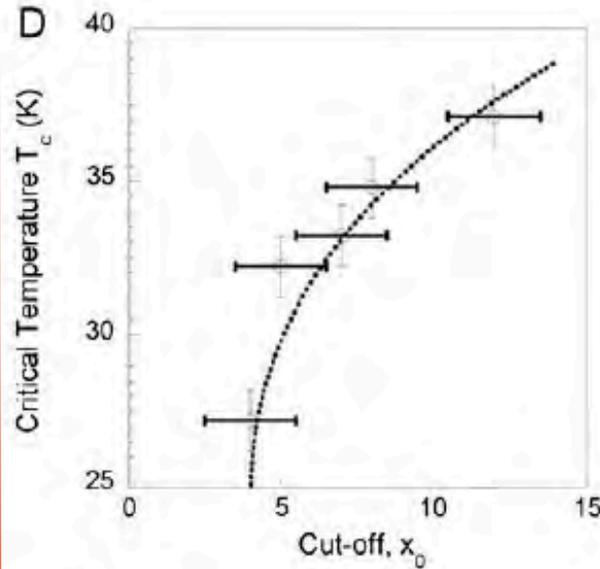
(A, B, C panels) µ-XRD results for the position dependence of the Q3-LLD superstructure intensity in La_2CuO_{4+y} crystals with different critical temperatures. Increasing Tc maps show the better self organization of LLD droplets.

(D) Tc in the range 25 K < Tc < 37 K for five samples vs. the cut-off parameter of the power law distribution of the LLD droplets density.

La_2CuO_{4+y} actually contains networks of superconductors characterized by different ordered defects (Oi and LLD).
The best fractal behavior and superconductivity is obtained simultaneously for both Oi and LLD order. Furthermore, strains in the LLD droplets are correlated over the longest distances when stresses produced over still larger distances by the ordered interstitials, display their maximal correlations. This condition yields to superconductivity with the maximum Tc. Data point out that the complexity of the underlying material determines the value of Tc.

In La_2CuO_{4+y} at least 2 relevant networks of ordered defects coexist. However, more than 2 networks may occur in this and other more complex materials.

Zakopane, May 19, 2015

LLD droplets form networks whose nature varies with the superconducting critical temperature. µ-XRD can be used to map the evolution of the Q3-LLD satellites. On the right panels the probability distribution of XRD Q3-LLD intensities and the spatial correlation function, calculated for the intensities at the spots Rk.

All probability distributions of XRD intensities of the five single crystals of electrochemically doped La_2CuO_{4+y}, from the underdoped state (y = 0.06) to the optimum doping range 0.1 < y < 0.12, scale with the same power-law exponent α but with a variable cutoff in the range from 4.5 to 15 (A). The spatial correlation function of the underdoped sample with Tc = 27 K follows a power law, with the exponent η = 0.3 and a correlation length ξ = 30.

All power law distribution curves collapse on the same curve as a function of x/x0. Also the spatial correlation function G(r) of the Q3-LLD XRD (B) follows a power law distribution and as a function of r/ξ, collapse in a unique curve.

The susceptibility response of the single crystal of LaCuO with a small applied ac magnetic field, collected warming the sample from 4.4 K. The first harmonic (real part) χ_1' and the modulus of the third harmonic of ac susceptibility χ_3 of the underdoped $La_2CuO_{4.06}$ sample clearly show two phases: $Tc_1 \sim$ 14 K and $Tc_2 \approx$ 27 K.

Zakopane, May 19, 2015
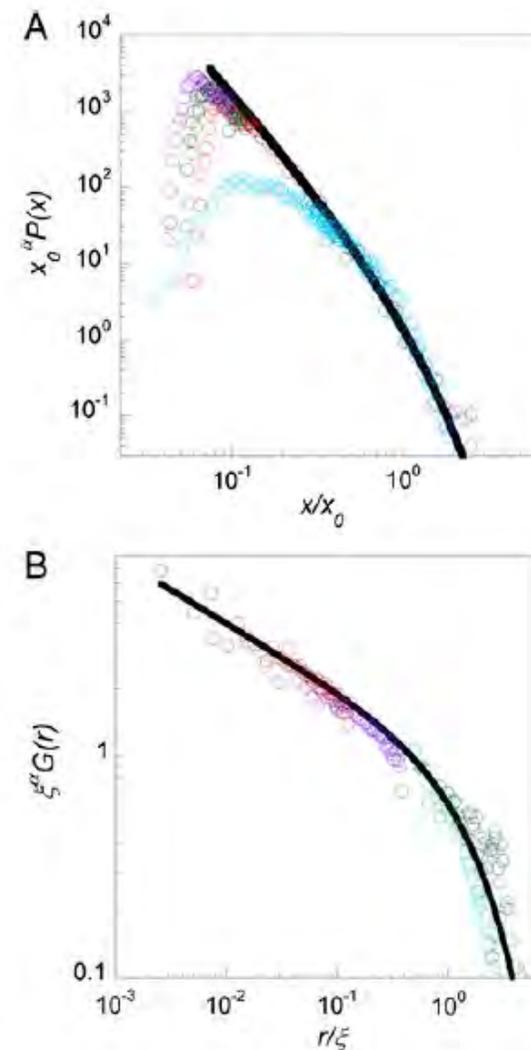
N. Poccia, M. Chorro, A. Ricci, Wei Xu, A. Marcelli, G. Campi and A. Bianconi
Percolative superconductivity in $La_2CuO_{4.06}$ by lattice granularity patterns with scanning micro x-ray absorption near edge structure
Applied Physics Letters 104, 221903 (2014)

µ-XANES measurements were performed using LUCIA at SOLEIL with the high brilliance (1.6 10^{11} ph/s/400 mA) Apple II-UH52 undulator soft X-rays source (0.8–8 keV). The polarized monochromatic photon beam was focused with a couple of KB mirrors on a 2.5 x2.5 µm^2 spot. At each x-z position, the lanthanum L$_3$-edge XANES signal was recorded in the fluorescence mode with a 4 elements Si drift Bruker detector.
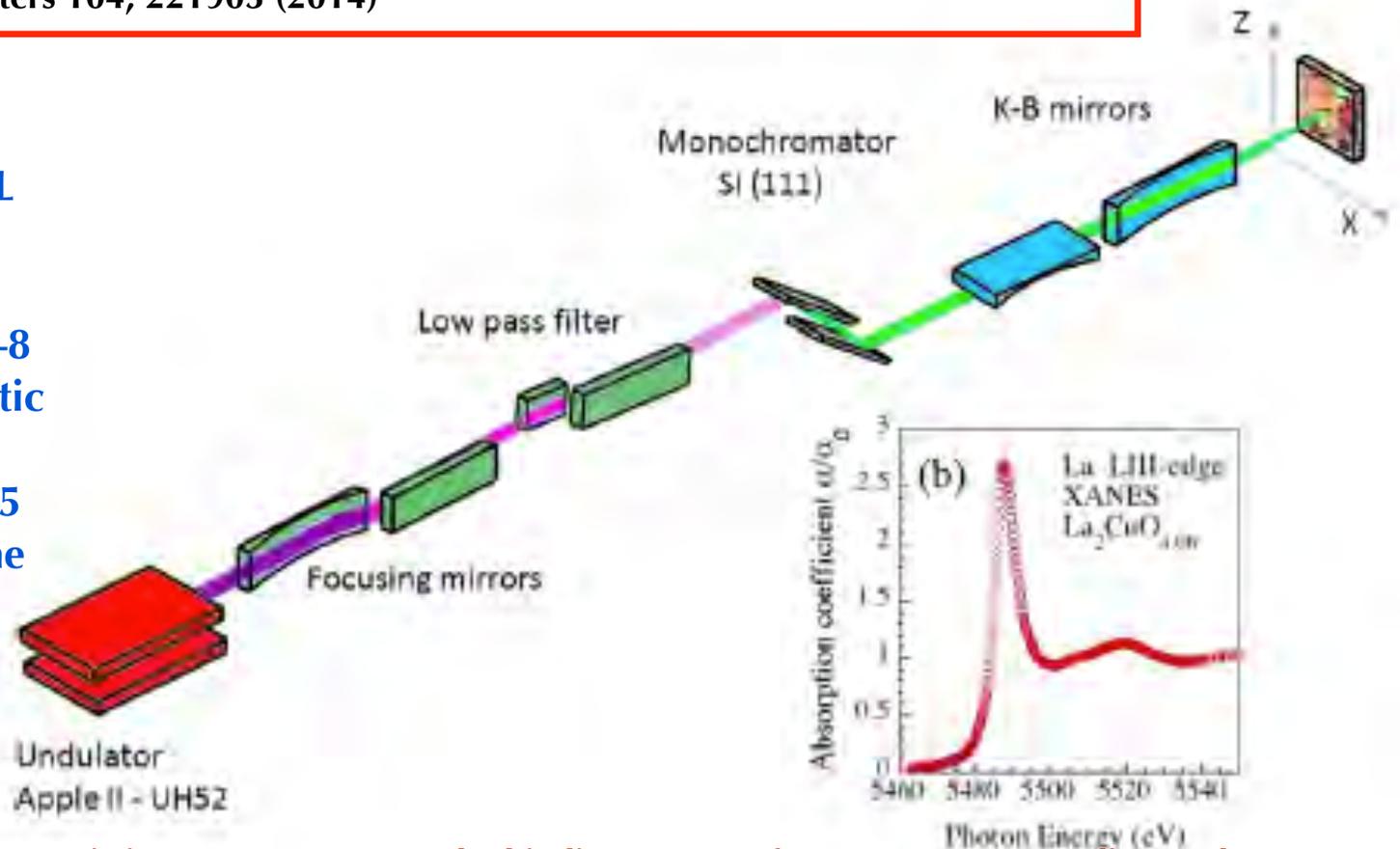
Characteristic La L$_3$ spectrum at the binding energy of 5383 eV corresponding to the electronic transition from the 2p level to 5d empty states.

Zakopane, May 19, 2015

The behavior of the atomic absorption, due to electronic transitions from the atomic La $(2p)_{3/2}$ core level to the continuum, times the modulation of the atomic absorption cross section, extracted by subtracting the atomic absorption from the experimental spectrum. The atomic absorption spectrum has been obtained by fitting the experimental XANES spectrum with an arctangent in a range of 10 eV below the absorption edge and in the range between 15 and 20 eV above the absorption edge.

In the upper panel are compared two La L_3-edge XANES spectra (blue and red dots) recorded at two different spots of the crystal. The black dashed line is the atomic absorption. Black circles shows the difference between the experimental absorption and the atomic absorption while the black continuous curve is the fit of the shape resonance by a Fano lineshape curve.

In the lower panel the difference between XANES spectra recorded in two different spots (i.e., two 2.5x2.5 μm^2 pixels) is well beyond the error bar and resembles the shape resonance. XANES differences measured in the real space are determined by the variation of the shape resonance in different areas as probed by the spot.

Lanthanum L_3-edge in $La_2CuO_{4.06}$

Zakopane, May 19, 2015
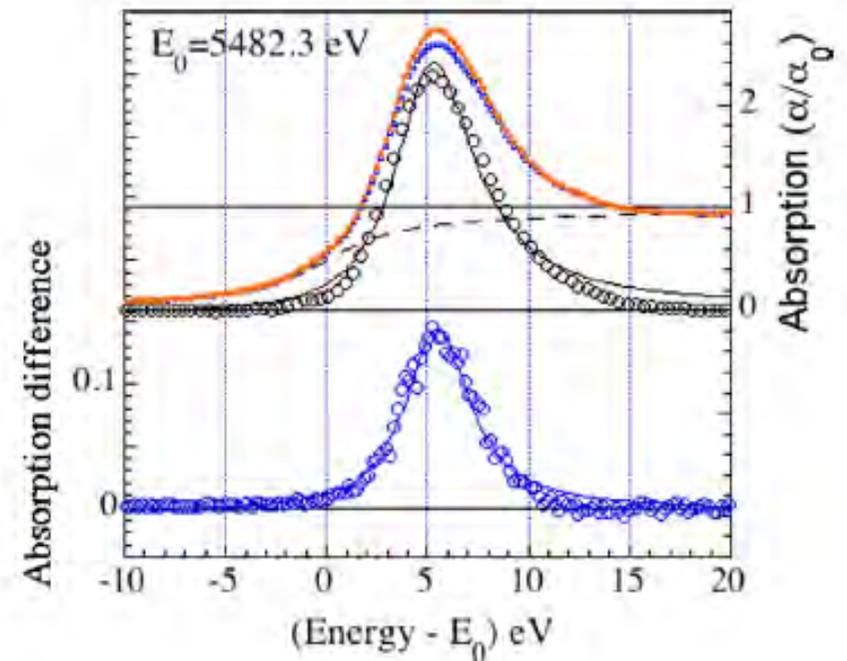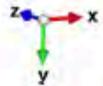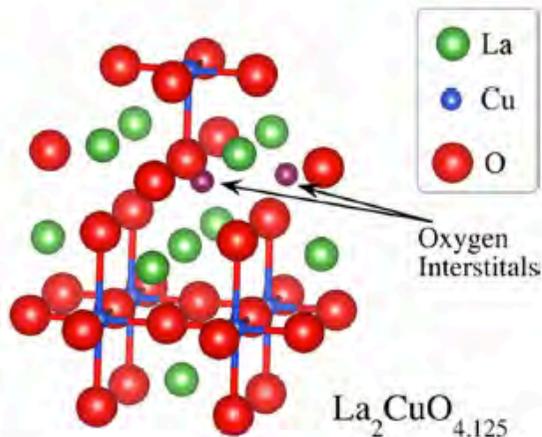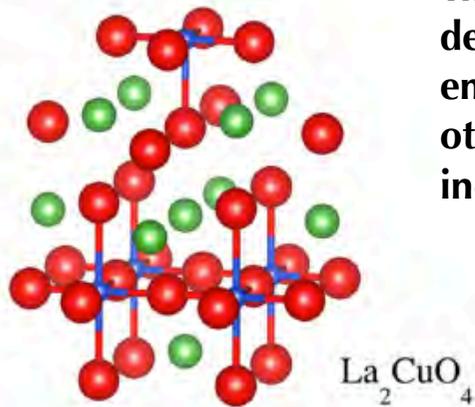
The atomic cluster (~8 Å) surrounding La (green) in a La_2CuO_{4+y} crystal that determines the shape resonance in the La L_3-XANES. The photoelectron wave emitted by the absorbing atoms are scattered by Cu (blue), oxygens (red) and other La ions. In oxygen rich puddles (as in the $La_2CuO_{4.125}$ crystal) the cluster includes additional Oi (purples spheres indicated by the arrows).

FMS La L_3 XANES calculation for the La_2CuO_4 (brown) and the $La_2CuO_{4.125}$ (black). In the bottom the difference between the two spectra. As shown in the lower panel, Oi induce an increase of the peak due to the first and strongest MSR.

The superimposition of two XANES spectra in the ORPs (La_2CuO_{4+y} with y~0.125 Oi) and in the OPP (La_2CuO_4 without Oi with y~0) shows an increase by 0.4 in units of the La L_3-edge atomic absorption jump and a shift of the white-line in correspondence of the ORP.

FMS theory
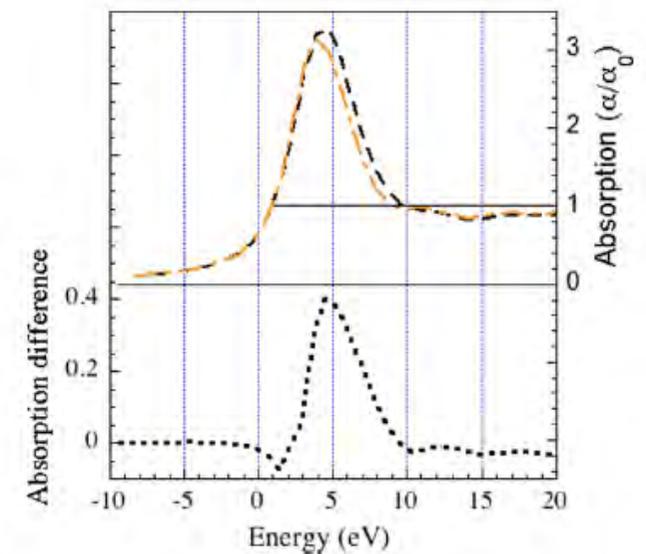
Zakopane, May 19, 2015

Color maps of the position dependent intensity of the MSR in the XANES spectra of the $La_2CuO_{4.06}$ crystal. Maps are 36x18 pixels (4 μm pixel size). The exposition time was 10 s/step. In (c) are compared the probability density function PDF(x) of the MSR of the **ORP** and **OPP** regions.

We reconstructed the intensity of the main MSR peak in the XANES spectra using a spot of 4 μm. The spatial distribution of ORPs and OPPs is revealed looking at the MSR peak and comparing the images where different spatial distributions of ORP occur.

The statistical analysis, i.e., the distribution curves of the two regions are shown in panel (c). The x axis is the intensity of the MSR, which ranges from 2.4 to 2.7 in units of the absorption jump. The Gaussian distribution of the map (a) peaked at 2.6 while the map (b) at 2.5 [see panel (c)]. **The width of the oxygen poor distribution (OPP) ranges from 2.45 to 2.55**, while for the **oxygen rich region (ORP) it ranges from 2.52 to 2.65**, i.e., we have different distributions in different locations.

The variation of the MSR intensity is smaller respect to the calculation. Actually, as showed by scanning μ-XRD experiments, **OPP** regions are <4 μm and, at SOLEIL, with their micro-beam it was impossible to probe regions free from **ORPs**.
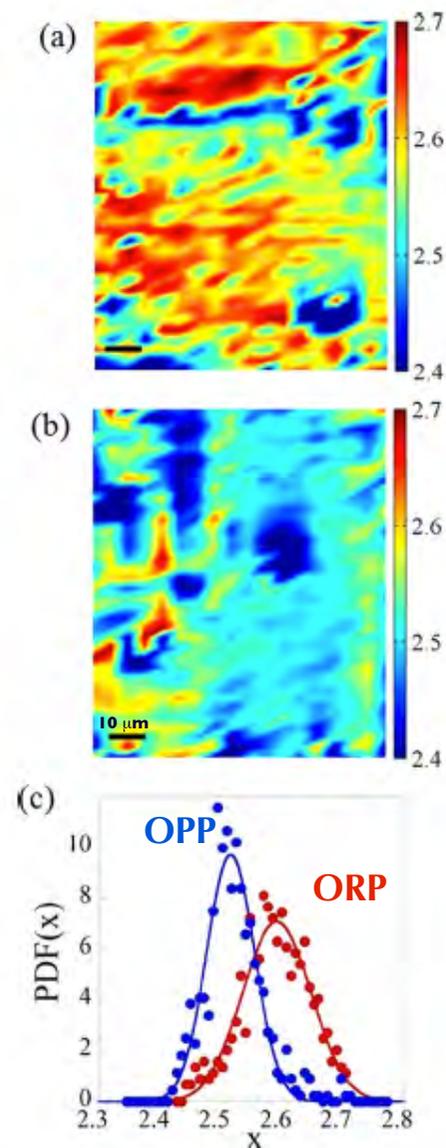
Thanks to SR optical layouts, X-ray imaging at high spatial resolution can be combined with μ-XANES spectroscopy to reconstruct 2D and 3D morphological and chemical changes in large volumes from sub-μm to tens of nanometers resolution. μ-XANES data of La_2CuO_{4+y}, the simplest cuprate superconductor with mobile oxygen interstitials, show a bulk multiscale structural phase separation in agreement with μ-XRD. μ-XANES mapping at the La L_3-edge provides support to a percolative superconductivity scenario in copper oxides and other HTc cuprates superconductors. Indeed, the percolation phenomenon strongly affect the superconducting properties within different theoretical frameworks that point out the intrinsic percolative nature of the superconductivity phenomenon.


The temperature-dependent complex surface resistivity of the underdoped $La_2CuO_{4+\upsilon}$ crystal (blue) and its derivative (red) showing two critical temperatures $Tc_1 \sim 27$ K and $Tc_2 \sim 13$ K.

$La_2CuO_{4+\upsilon}$ is a prototype of cuprate superconductors, showing a clear phase separation. Neutron powder diffraction already showed the occurrence of a phase separation and a miscibility gap between an antiferromagnetic phase at y=0.01 and a superconducting phase at y=0.055. The phase separation for y> 0.055 was object of discussion for long time. Neutron diffraction on single crystals at higher concentration of Oi provided evidence for superstructure satellites, but still there is a lack of information on the spatial location of multiple phases. An EXAFS experiment on a y=0.1 sample has shown local lattice fluctuations in the CuO_2 plane. Moreover, a large mobility of Oi occurs in this system. The spatial distribution of puddles with 3D ordered Oi can be described by scanning μ-XRD in an optimally doped $La_2CuO_{4.1}$ (Tc~40 K) and in an underdoped $La_2CuO_{4.06}$. Both experiments point out that Oi -rich puddles (ORP) form a scale-free network of superconducting puddles at the optimum doping, which favors the HTS.

Zakopane, May 19, 2015

Is superconductivity at higher temperatures possible?

By tuning a complex materials made of multiple-elements, multiple symmetries and a complex topology
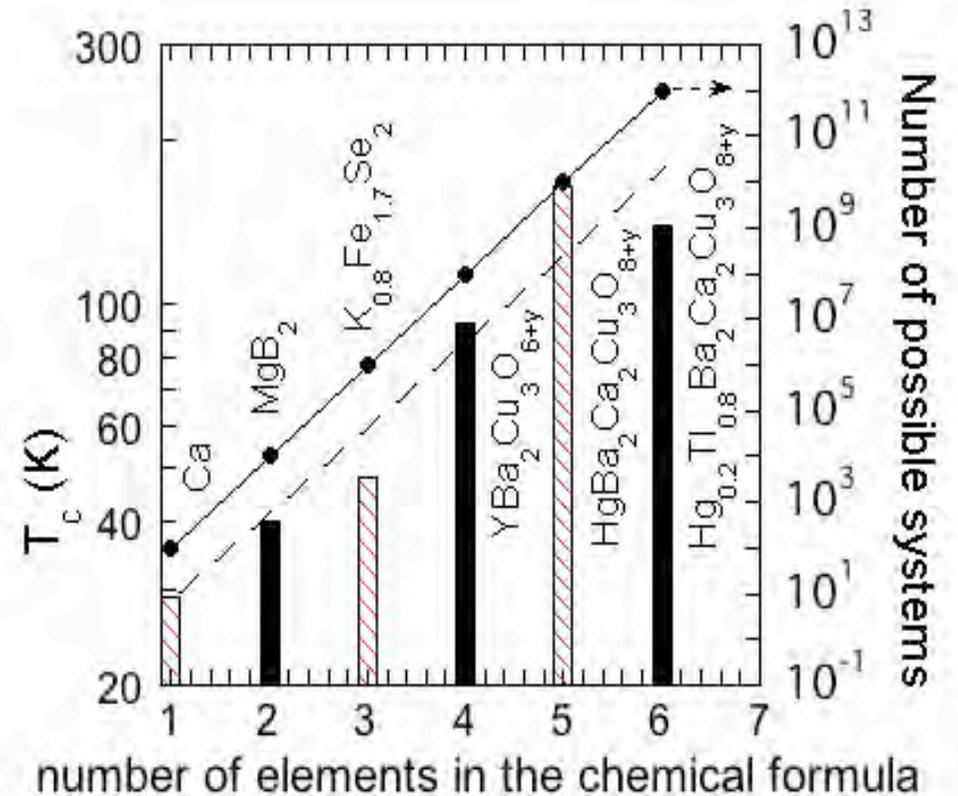
The new physics of this century is focusing to understand the intricate non trivial mesoscale inhomogeneity observed in heterogeneous materials where new low energy quantum physical phenomena are emerging.

The mesoscopic world separates the atomic scale (0.1-10 nm) from the macroscopic world (d>100 microns) but the energy differences among mesostructures is just few tens of meV!

Zakopane, May 19, 2015

Mesoscale Science

Mesoscale science, where atomic granularity, quantization of energy, and simplicity of structure and function give way to continuous matter and energy, complex structures, and composite functionalities, is a broad and rich horizon for innovative materials and chemistry.

We assisted to a continuous increase of investigations at ever smaller length and time scales that reveal the atomic, molecular, and nanoscale origins of macroscopic behavior. Now, we have to begun to reverse the approach, using the knowledge of nanoscale phenomena to understand and control mesoscale architectures to promote the emergence of new behaviors.

Actually the mesoscale is an inherently dynamic regime, where energy and information captured at the nanoscale are processed and transformed at the mesoscale. Experiments have to look at the dynamics, possibly *in situ*, and have to be multimodal being the ordinary "static" characterization not more sufficient.

Zakopane, May 19, 2015

Conclusions

- The μ-XANES technique is perfectly suited to visualize the nature of these multi-scale systems, being a fast and local probe of a selected atomic species;

- The μ-XANES is a complementary technique to scanning μ-XRD and provide further support to the scenario of percolative superconductivity in copper oxides and other HTC cuprates superconductors;

- The μ-XANES investigation of an underdoped cuprate oxide with mobile Oi dopants shows the existence of a spatial distribution of ORPs at the micron scale;

- The arrangement of ORPs in the real space shows a compelling evidence of different percolation regimes occurring in multi-scale systems;

- The occurrence of two (or more) critical temperatures supports different models based on the intrinsic percolative nature of the superconductivity mechanism not limited to low temperatures.

Zakopane, May 19, 2015

Acknowledgements

- DANIELE DI GIOACCHINO

- ANTONIO BIANCONI

- NICOLA POCCIA

- GAETANO CAMPI

- MATTHIEU CHORRO

- WEI XU

- ALESSANDRO RICCI

- ....

MARCELLI@LNF.INFN.IT

A) NANOSCALE PHASE SEPARATION

- Iron based superconductors
- Cuprates
- Colossal magnetoresistance
- Ferroelectrics, relaxors, memistors
- Complex magnetic materials

B) CDW

- in cuprates, organics, complex matter

C) ORBITAL EFFECTS

- Orbital density waves
- Spin-orbit coupled systems
- Isotope effect
- Jahn Teller Polarons
- Large Polarons

D) STRIPES IN HIGH Tc SUPERCONDUCTORS and COMPLEX MAGNETIC MATERIALS

- Charge stripes, Magnetic stripes, Superconducting stripes, Lattice Stripes

E) DEFECTS

- Quenched disorder (Dopants, Misfit Strain, corrugation, filaments, puddles, lattice distortion) in layered materials
- Incommensurate phases and quasi-crystals.

F) COMPLEX MAGNETIC STRUCTURE IN CUPRATES

- Magnetic quantum phase transition
- FFLO
- Spin spirals
- Magnetic structure of cuprates

F) CRITICAL POINTS

- Quantum criticality
- Griffiths phases and other rare region effects
- Effect of disorder on Phase Transitions

G) TOPOLOGICAL QUANTUM FIELD THEORY

in high temperature superconductivity

H) VORTEX MATTER

- Magnetoresistance
- Phase transitions

I) HIGH Tc AT HIGH PRESSURE

L) QUANTUM DEVICES

M) TIME RESOLVED DYNAMICS OF COMPLEX MATERIALS

N) NANOSCALE MATERIALS

- Graphene, fullerene-based,
- Aromatic superconductors
- Related carbon base materials

0) SILICENE and related materials

P) GRANULAR NANOSCALE SUPERCONDUCTORS

- Control and manipulation
- Fractal superconductivity

Q) SUPERCONDUCTOR-TO-INSULATOR TRANSITION AND EMERGENT INHOMOGENEITY

R) MULTI-COMPONENTS SUPERCONDUCTIVITY

- Multi-condensates superconductors
- Multi-gap superconductors
- Shape resonances in superconducting gaps
- Fermi-Bose systems
- Negative U Centers in multi-components materials

S) SUPERCONDUCTIVITY AT NANOSCALE

- Quantum size effects
- 2DEG in oxide interfaces
- Proximity effects

T) ELECTRONIC CRYSTALS

- Inhomogeneous electronic crystals

U) COMPLEX FERMIOLOGY of superconductors

- Multiband materials,
- Lifshitz transitions,
- Electronic Topological Transitions
- Cuprates with multiple Fermi surface spots
- Iron based superconductors
- Correlated electronic systems

V) NANOMAGNETISM

- Magnetic nanomaterials
- Single molecule magnetism

X) THERMOELECTRIC DEVICES

Y) MULTIFERROICS

Thanks

MARCELLI@LNF.INFN.IT